

Article

An RNA-Based Vaccine Platform for Use against *Mycobacterium tuberculosis*

Sasha E. Larsen ¹, Jesse H. Erasmus ^{2,3}, Valerie A. Reese ¹, Tiffany Pecor ¹, Jacob Archer ², Amit Kandahar ², Fan-Chi Hsu ⁴, Katrina Nicholes ², Steven G. Reed ², Susan L. Baldwin ¹ and Rhea N. Coler ^{1,5,6,*}

¹ Center for Global Infectious Disease Research, Seattle Childrens Research Institute, Seattle, WA 98109, USA

² HDT BioCorp, Seattle, WA 98102, USA

³ Department of Microbiology, University of Washington, Seattle, WA 98109, USA

⁴ Hematologics Inc., Seattle, WA 98121, USA

⁵ Department of Pediatrics, University of Washington, School of Medicine, Seattle, WA 98105, USA

⁶ Department of Global Health, University of Washington, Seattle, WA 98105, USA

* Correspondence: rhea.coler@seattlechildrens.org

Abstract: *Mycobacterium tuberculosis* (M.tb), a bacterial pathogen that causes tuberculosis disease (TB), exerts an extensive burden on global health. The complex nature of M.tb, coupled with different TB disease stages, has made identifying immune correlates of protection challenging and subsequently slowing vaccine candidate progress. In this work, we leveraged two delivery platforms as prophylactic vaccines to assess immunity and subsequent efficacy against low-dose and ultra-low-dose aerosol challenges with M.tb H37Rv in C57BL/6 mice. Our second-generation TB vaccine candidate ID91 was produced as a fusion protein formulated with a synthetic TLR4 agonist (glucopyranosyl lipid adjuvant in a stable emulsion) or as a novel replicating-RNA (repRNA) formulated in a nanostructured lipid carrier. Protein subunit- and RNA-based vaccines preferentially elicit cellular immune responses to different ID91 epitopes. In a single prophylactic immunization screen, both platforms reduced pulmonary bacterial burden compared to the controls. Excitingly, in prime-boost strategies, the groups that received heterologous RNA-prime, protein-boost or combination immunizations demonstrated the greatest reduction in bacterial burden and a unique humoral and cellular immune response profile. These data are the first to report that repRNA platforms are a viable system for TB vaccines and should be pursued with high-priority M.tb antigens containing CD4+ and CD8+ T-cell epitopes.

Keywords: *Mycobacterium tuberculosis*; ID91; GLA-SE; repRNA; nanostructured lipid carrier; tuberculosis; vaccine



Citation: Larsen, S.E.; Erasmus, J.H.; Reese, V.A.; Pecor, T.; Archer, J.; Kandahar, A.; Hsu, F.-C.; Nicholes, K.; Reed, S.G.; Baldwin, S.L.; et al. An RNA-Based Vaccine Platform for Use against *Mycobacterium tuberculosis*. *Vaccines* **2023**, *11*, 130. <https://doi.org/10.3390/vaccines11010130>

Academic Editor: Jorge H. Leitão

Received: 25 October 2022

Revised: 21 December 2022

Accepted: 28 December 2022

Published: 5 January 2023



Copyright: © 2023 by the authors. Licensee MDPI, Basel, Switzerland. This article is an open access article distributed under the terms and conditions of the Creative Commons Attribution (CC BY) license (<https://creativecommons.org/licenses/by/4.0/>).

1. Introduction

For the first time in a decade, 2020 saw an increase in annual deaths (1.5 million total) caused by *Mycobacterium tuberculosis* (M.tb) [1–3]. Before the Coronavirus disease 2019 (COVID-19) pandemic, caused by severe acute respiratory syndrome coronavirus 2 (SARS-CoV-2) [4], M.tb was the world's top cause of death from an infectious disease [5], regaining this title in 2022, with a reported 1.6 million deaths from M.tb [6]. Exposure to M.tb can result in productive infection and pulmonary tuberculosis disease (TB). COVID-19-pandemic-related disruptions in TB care and case finding are estimated by the World Health Organization (WHO) to lead to a further half-million preventable TB deaths [7]. This dual assault from respiratory pathogens is most heavily felt by low- and middle-income countries (LMICs), which endure a disproportionate burden of TB disease [8] and are also suffering from a lack of access to vaccines for SARS-CoV-2 [9]. Moreover, within M.tb, drug resistance is steadily increasing globally. For the past five years, nearly 0.5 million patients infected with M.tb annually develop resistance to front-line antibiotic rifampicin and approximately 80% of those harbor multidrug resistance [1,2,5]. Novel antibiotic regimens [10–14] are

being developed but many models are insufficient alone to combat this epidemic [15,16]. Specifically designed low-cost and effective TB vaccines for the prevention of infection (POI) or the complementary prevention of active disease (POD) endpoints are desperately needed [17].

While clinical trials suggest that *Mycobacterium bovis* bacille Calmette-Guérin (BCG) may prevent M.tb infection in adolescents [18], and subunit adjuvanted vaccine candidate M72/AS01_E [19,20] prevents TB disease in a subset of interferon-gamma release assay (IGRA)-positive individuals, there is no currently approved vaccine for POI or POD in adults. This lag is partially due to the fact that the financial resources available for testing drug and vaccine candidate regimens in human clinical settings are disproportionately low for TB relative to the global burden of the disease. Addressing the improved efficacy of prophylactic vaccines against M.tb and the supply and costs of manufacturing materials are all required to ensure that a vaccine is readily available to those who need it. Thankfully, renewed enthusiasm for TB vaccine research has been stimulated largely by two main pillars of preclinical and clinical advancements. First, the pursuit of correlates of protection against TB, which are refining the immune players in the fight against infection and disease, and second, the pursuit of cutting-edge vaccine delivery platforms.

Historically the vaccine pipeline has relied on CD4+ T helper 1 (TH1) type responses as a benchmark for the immunogenicity stage-gating of vaccine candidates. However, the full mechanism of protection has yet to be determined [21], and several preclinical and clinical reviews suggest that the CD4+ TH1 subset producing proinflammatory cytokine IFN γ alone is not sufficient nor fully predictive of clinical efficacy [22–25]. Indeed, protection from M.tb infection and TB disease is likely a multifaceted process involving many cell types beyond canonical CD4+ T cells, and our focus here is on M.tb-antigen-specific CD8+ T cells. Many reviews are devoted to the significance of CD8+ T cells in TB infection and disease [26–31], yet still, they are not prioritized as a vaccine target cell type in most candidate screens. Importantly, CD8+ T cells can migrate to the site of M.tb infection [32–34], and removing MHC class I or CD8+ T cells in vivo enhances M.tb susceptibility [29,35–38]. Cytolytic CD8+ T cells produce IFN γ , a key proinflammatory cytokine known to help control M.tb and lyse M.tb-infected macrophages [39–42]. Due to their ability to home to pulmonary spaces and anti-M.tb-effector functions, it is unsurprising that in preclinical models of an M.tb challenge, CD8+ T cells help reduce bacterial burden [26,29,33,43]. Most recently, the use of intravenous (i.v.) BCG vaccination in nonhuman primates (NHP) has provided a benchmark of immune responses that correlated with nearly sterilizing protection from an M.tb challenge [44]. Notably, in the routine intradermal (i.d.) BCG vaccine NHP cohort, there was a lack of proinflammatory CD8+ T cells and less protection when compared to i.v. BCG [44]. These data collectively suggest that CD8+ T cells represent an underappreciated target for vaccine-induced efficacy endpoints.

Many strategies designed to induce robust anti-M.tb CD8+ T cells have been developed and are well-reviewed here [26,27,31]. Some examples include recombinant BCG (VPM1002), chimpanzee adenoviral vectored strategies (ChAdOx185A), modified vaccinia virus Ankara (MVA85A), recombinant adenoviruses (Ad5Ag85A, AERAS-402), and Cytomegalovirus vector approaches (CMV-6Ag and MTBVAC) and are under clinical evaluation [21,26,27,45,46]. Interestingly, a majority of these candidates are vector- or replication-based. Enriching the pipeline with novel candidates and platforms is warranted, given the expanding immune correlates being discovered and the need for broad accessibility in LMICs. Leveraging RNA vaccines, for example, circumvents the challenges of protein manufacturing, reducing vaccine development timelines from several years to months and reducing costs throughout pipeline evaluations and deployment. For example, once the SARS-CoV-2 sequence was made available publicly, messenger RNA (mRNA) vaccines were developed within months and tested in human clinical trials [47]. While RNA vaccine platforms have been very minimally leveraged for TB vaccines [48] in pre-clinical efficacy testing to our knowledge, the evidence for targeting multifaceted immune responses against M.tb for high vaccine efficacy provides a good rationale for evaluating

this platform. Indeed BioNTech (Mainz, Germany) has recently announced the initiation of a phase-one clinical trial for the safety testing of an mRNA TB vaccine candidate in collaboration with the Bill and Melinda Gates Foundation (ClinicalTrials.gov Identifier: NCT05547464). We and others have previously demonstrated robust humoral and cellular responses, including CD8+ T-cell responses, induced by replicating RNA delivered via multiple different modalities [49–52]. For these reasons, we designed and evaluated a novel replicating RNA platform (repRNA) [49] both as a homologous TB vaccine and as a heterologous strategy to complement protein–adjuvant prophylactic vaccine candidates against an *M.tb* challenge in mice. We hypothesize that the replicating aspect of repRNA, resulting in longer antigen exposure [49] more similar to BCG than protein–adjuvant strategies, will enhance immune responses against selected *M.tb* vaccine candidate antigens.

2. Materials and Methods

ID91 repRNA production and qualification. The codon-optimized sequence encoding ID91 was synthesized (Codex DNA) and cloned into the Venezuelan equine encephalitis virus replicon (strain TC83) between PflFI and SacII sites using a Gibson assembly. The sequence-verified DNA was then linearized by NotI digestion and RNA transcribed and capped by T7 RNA polymerase and Vaccinia capping enzyme reactions, respectively, as previously described [50]. To validate the ID91 repRNA produced ID91 protein, Baby Hamster Kidney (BHK) cells (ATCC) were transfected with 4 µg ID91-repRNA or GFP-repRNA as a negative control using lipofectamine 2000 (ThermoFisher, Waltham, MA, USA). After 24 h, the cells and supernatants were collected for analysis by SDS-PAGE and Western blot under reducing conditions. Included in the blot were ID91 protein control and MagicMark XP ladder (Thermo Fisher). For ID91 antigen detection after the transfer to the PVDF membrane, primary mouse sera (from animals immunized 3 times 3 weeks apart with ID91 + GLA-SE) was used at 1:500 in PBS. Goat anti-mouse HRP (SouthernBiotech) 1:10000 was used for detection along with SuperSignal™ West Pico PLUS Chemiluminescent Substrate (ThermoFisher). The resulting image was captured on a Biorad chemidoc XRS+.

Preclinical animal model. Female C57BL/6 mice 4–6 weeks of age were purchased from Charles River Laboratory. The mice were housed at the Infectious Disease Research Institute (IDRI) biosafety level 3 animal facility under pathogen-free conditions and were handled in accordance with the specific guidelines of the IDRI Institutional Animal Care and Use Committee. The institute, formerly known as IDRI, operated under USDA Certificate # 91-R-0061 and PHS Assurance # A4337-01. The mice were infected either with a low-dose (50–100 bacteria) aerosol (LDA) or ultra-low dose (1–8 bacteria) aerosol (ULDA) of *M.tb* H37Rv using a University of Wisconsin-Madison aerosol chamber. Twenty-four hours post-challenge, the lungs of 3 mice were homogenized and plated on Middlebrook 7H11 agar (Fisher Scientific) to confirm delivery.

Vaccines and adjuvants. The cohorts of mice were immunized intramuscularly (i.m.) twice three weeks apart for epitope mapping, once 6 weeks before the challenge, or twice three weeks apart, with the final immunization occurring 3 weeks before the challenge for immunogenicity and efficacy testing. The mice received either saline alone or vaccinations containing 0.5 µg/dose of ID91 recombinant fusion protein combined with 5.0 µg/dose GLA-SE, as previously published [53–55]. A separate cohort of mice was immunized with 1.0 µg repRNA complexed with NLC, as described [49]. Homologous or heterologous regimens were also leveraged using the doses and regimens outlined above. Combination cohorts received ID91 + GLA-SE in the right hind limb followed by ID91 repRNA + NLC in the left hind limb at both prime and boost time points in the same doses described above.

Epitope mapping: Two weeks post-boost, the splenocytes were isolated from the cohorts of ID91 + GLA-SE or ID91 repRNA + NLC-immunized mice and stimulated with ID91 protein antigen (10 µg/mL), overlapping peptides (10 µg/mL), or media alone for 60 h at 37 °C and 5% CO₂ with proliferation dye (Violet Proliferation Dye, BD Biosciences). The peptides were generated in the 15 mer format with 8 amino acid overlaps for the ID91 fu-

sion antigen, for a total of 125 peptides (BioSynthesis). These 125 peptides make up 13 different pools of 5–10 peptides each (Table 1). Cells were then restimulated for two hours, brefeldin A was added directly to the plate and cells were allowed to incubate for a further 4 h. The cells were then washed, and ICS and flow cytometry analysis were performed, as described below.

Table 1. ID91 peptide pool composition used for peptide stimulation of splenocytes.

| | | | | | |
|----|------------------|----|------------------|-----|-------------------|
| | Pool 1 | 43 | AAAAYETAYRLTVPPP | 86 | PGLPVEYLQVPSPSM |
| 1 | HMTINYQFGDVDAHG | 44 | YRLTVPPPVIAENRT | 87 | LQVPSPSMGRDIKVQ |
| 2 | FGDVDAHGAMIRAQA | 45 | PVIAENRTELMTLTA | 88 | MGRDIKVQFQSGGNN |
| 3 | GAMIRAQAGSLEAEH | 46 | TELMTLTATNLLGQN | 89 | QFQSGGNNSPAVYLL |
| 4 | AGSLEAEHQAIISDV | 47 | ATNLLGQNTPAIEAN | 90 | NSPAVYLLDGLRAQD |
| 5 | HQAIISDVLTASDFW | 48 | NTPAIEANQAAYSQM | | Pool 10 |
| 6 | VTASDFWGGAGSAA | 49 | NQAAYSQMWWQDAEA | 91 | LDGLRAQDDYNGWDI |
| 7 | WGGAGSAACQGFITQ | 50 | MWQDAEAMYGAAAT | 92 | DDYNGWDINTPAFEW |
| 8 | ACQGFITQLGRNFQV | | Pool 6 | 93 | INTPAFEWYYSGLS |
| 9 | QLGRNFQVIYEQANA | 51 | AMYGYAATAATATEA | 94 | WYYQSGLSIVMPVGG |
| 10 | VIYEQANAHGQKVQA | 52 | TAATATEALLPFEDA | 95 | SIVMPVGGQSSFYSYD |
| | Pool 2 | 53 | ALLPFEDAPLITNPG | 96 | GQSSFYSYDWYSPACG |
| 11 | AHGQKVQAAGNNMAQ | 54 | APLITNPGGLLEQAV | 97 | DWYSPACGKAGCQTY |
| 12 | AAGNNMAQTDSAVGS | 55 | GGLLEQAVAVEEAID | 98 | GKAGCQTYKWETFLT |
| 13 | QTDSAVGSSWADDID | 56 | VAVEEAIDTAAANQL | 99 | YKWETFLTSELQPWL |
| 14 | SSWADDIDWDAIAQC | 57 | DTAAANQLMNNVPQA | 100 | TSELQPWLSANRAVK |
| 15 | DWDAIAQCESGGNWA | 58 | LMNNVPQALQLAQF | | Pool 11 |
| 16 | CESGGNWAANTGNGL | 59 | ALQQLAQPAQGVVPS | 101 | LSANRAVKPTGSAAI |
| 17 | AANTGNGLYGLQIS | 60 | PAQGVVPSKLGGLW | 102 | KPTGSAAIGLSMAGS |
| 18 | LYGGLQISQATWDSN | | Pool 7 | 103 | IGLSMAGSSAMILAA |
| 19 | SQATWDSNGGVGSPA | 61 | SSKLGGLWTAVSPHL | 104 | SSAMILAAYHPQQFI |
| 20 | NGGVGSPAASPQQQ | 62 | WTAVSPHLSPLSNVS | 105 | AYHPQQFIYAGLSLA |
| | Pool 3 | 63 | LSPLSNVSSIANNHM | 106 | IYAGLSLALLDPSQG |
| 21 | AAASPQQQIEVADNI | 64 | SSIANNHMSMMGTGV | 107 | ALLDPSQGMGPSLIG |
| 22 | QIEVADNIMKTQGP | 65 | MSMMGTGVSMNTLH | 108 | GMGPSLIGLAMGDAG |
| 23 | IMKTQGPRAWPKCSS | 66 | VSMTNTHSMLKGLA | 109 | GLAMGDAGGYKAADM |
| 24 | GAWPKCSSCSQGDAP | 67 | HSMLKGLAPAAAQAVE | 110 | GGYKAADMWGPSSDP |
| 25 | SCSQGDAPLGLSLTHI | 68 | PAAAQAVETAENG | | Pool 12 |
| 26 | PLGLSLHILTFLAEE | 69 | ETAENGVMWAMSSLG | 111 | MWGPSSDPAWERNDP |
| 27 | ILTFLAETGGCSGS | 70 | VWAMSSLSQLGSSL | 112 | PAWERNDPQIPKL |
| 28 | ETGGCSGRDDVVDF | | Pool 8 | 113 | PTQIPKLVANNTRL |
| 29 | SRDDVVDFGALPPEI | 71 | CSQLGSSLGSSGLGA | 114 | LVANNTRLWVYCGNG |
| 30 | FGALPPEINSARMYA | 72 | LGSSGLGAGVAANLG | 115 | LWVYCGNGTNPENLGG |
| | Pool 4 | 73 | AGVAANLGRAASVGS | 116 | GTPNELGGANIPAEF |
| 31 | INSARMYAGPGSASL | 74 | GRAASVGSLSVPPAW | 117 | GANIPAEFLENFVRS |
| 32 | AGPGSASLVAAAKMW | 75 | SLSVPPAWAAANQAV | 118 | FLENFVRSSNLKFQD |
| 33 | LVAANKMWDSVASDL | 76 | WAAANQAVTPAARAL | 119 | SSNLKFQDAYNAAGG |
| 34 | WDSVASDLFSAASAF | 77 | VTPAARALPLTSLTS | 120 | DAYNAAGGHNAVFNF |
| 35 | LFAASAFQSVVWGL | 78 | LPLTSLTSAQAQTPG | | Pool 13 |
| 36 | FQSVVWGLTVGSWIG | 79 | SAAQTPAGHMLGGLP | 121 | GHNAVFNEPPNGTHS |
| 37 | LTVGSWIGSSAGLMA | 80 | GHMLGGLPLGHVNA | 122 | FPPNGTHSWEYWGAQ |
| 38 | GSSAGLMAAASPYPV | | Pool 9 | 123 | SWEYWGAQLNAMKGD |
| 39 | AAAASPYVAVMSVTA | 81 | PLGHVSNAGSGINNA | 124 | QLNAMKGDQLQSSSLGA |
| 40 | VAVMSVTAAGQAQLTA | 82 | AGSGINNALRVPARA | 125 | AMKGDQLQSSSLGACKL |

Table 1. Cont.

| | | | | | |
|----|-----------------|----|-----------------|----|---------------|
| | Pool 1 | 43 | AAAYETAYRLTVPPP | 86 | PGLPVEYLQVPSM |
| | Pool 5 | 83 | ALRVPARAYAIPTP | | |
| 41 | AGQAQLTAAQVRVAA | 84 | AYAIPTPAAGFSRP | | |
| 42 | AAQVRVAAAAYETAY | 85 | PAAGFSRPGLPVEYL | | |

Peptides composing ID91 fusion antigen: Rv3619 (brown), Rv2389 (green), Rv3478 (blue), and Rv1886 (red).

Flow cytometry. Intracellular flow cytometry was performed on the splenocytes post-immunization, but the pre-challenge and lung homogenates post-infection. The samples were incubated, washed, and stimulated, as previously described [54]. The cells were stimulated with media alone, 10 µg/mL of recombinant ID91, or 1 µg/mL phorbol myristate acetate (PMA) (Calbiochem) +1 µg/mL ionomycin (Sigma-Aldrich). Some sample stimulations also contained fluorescently labeled anti-mouse CD107a (1D4B, BioLegend). After stimulation, the samples were stained for markers of interest using fluorescent-conjugated antibodies, as previously described [54]. Notably, all of the sample stains were used at 10 µL/mL concentration. The primary surface staining included: anti-mouse CD4 (clone RM4-5, BioLegend), CD8a (clone 53-6.7, BioLegend), CD44 (clone IM7, eBioscience), CD154 (clone MR1, BioLegend), and 1 µg/mL of Fc receptor block anti-CD16/CD32 (clone 93, eBioscience) in PBS with 1% bovine serum albumin (BSA). The cells were then washed and fixed using BD Biosciences Fix/Perm reagent for 20 min at RT. Intracellular staining was carried out in Perm/Wash (BD Biosciences) reagent with anti-mouse GMCSF (clone MP1-22E9, BioLegend), IFN-γ (clone XMG1.2, Invitrogen), IL-2 (clone JES6-5H4, eBioscience), IL-17A (clone Tc11-1BH10.1, BioLegend), TNF-α (clone MP6-XT22, eBioscience), and IL-21 (mhalx21, eBiosciences) for 10 min at RT. The samples were then incubated in 4% paraformaldehyde for 20 min to fix, decontaminate, and remove from the containment facility before washing and resuspension in PBS + 1% BSA. An LSRFortessa flow cytometer (BD Bioscience) was used for sample acquisition, and analysis was performed using FlowJo v10.

Endpoint titer (EPT) ELISA. The serum was collected from terminal bleeds immediately after euthanasia at the post-boost or post-infection time points. Bronchoalveolar lavage fluid (BALf) was collected at the post-infection time points immediately after euthanasia. The serum samples were diluted to 1:100, and the BALf samples were added directly (neat) to plates coated with 2 µg/mL of ID91, Rv1886, Rv2389, Rv3478, or Rv3619. After overnight incubation, the plates were exposed to HRP-conjugated anti-IgA, Total IgG, IgG1, or IgG2c (Southern Biotech). The plates were then developed with a tetramethylbenzidine substrate and stopped with 1 N H₂SO₄. The plates were read at 450 nm with 570 nm background subtraction. The EPTs were calculated using a regression analysis of the sample dilution and O.D. on GraphPad Prism.

Bacterial burden/Colony-forming units (CFU). Then, 24 h to 3 weeks post-infection with *M.tb*, 3–7 mice per group were euthanized using CO₂. The lung and spleen tissue from the infected animals was isolated and homogenized in 5 mL of either RPMI + FBS (lung) or PBS+ Tween-80 (Sigma-Aldrich, St. Louis, MO, USA) CFU buffer (spleen) using an Omni tissue homogenizer (Omni International, Kennesaw, GA, USA). Serial dilutions of homogenate were made in CFU buffer, and the aliquots were plated on Middlebrook 7H11 agar plates and subsequently incubated at 37 °C and 5% CO₂ for 2–3 weeks before the colonies were counted. Bacterial burden, as CFU/mL, was calculated per organ and is presented here as Log₁₀ values. Reduced bacterial burden was calculated as the difference in the mean Log₁₀ values between the groups assessed.

Statistics. The number of animals included in the efficacy studies ($n = 7$ mice/group) is required to provide a statistical power of 95% with an alpha (p -value) of 0.05 to detect a significant difference in the bacterial burden between the groups by the CFU-plating of the lung homogenates post-challenge. The bacterial burden and humoral and cellular immune responses were assessed using a One-way ANOVA with Dunnett's multiple comparison test between the vaccinated groups and the saline control. The flow cytometry data were

assessed using FlowJo v10 (BD), and SPICE (NIH) using the Wilcoxon signed rank test as compared to the untreated groups or One-way ANOVA with Dunnett's multiple comparison test. Statistical analyses were performed using GraphPad Prism 7 software. Significant differences are labeled accordingly in the figures where * $p < 0.05$, ** $p < 0.01$, *** $p < 0.001$, and **** $p < 0.0001$, with the methodology used previously by our group [54,56].

3. Results

3.1. *M.tb* RNA Candidate Vaccine

The preclinical *M.tb* vaccine candidate ID91 is a fusion of four *M.tb* proteins: Rv3619 (esxV; ESAT6-like protein), Rv2389 (RpfD), Rv3478 (PPE60), and Rv1886 (Ag85B) (Figure 1A). These antigens were selected as candidates for *M.tb* vaccines based on their lack of human-sequence homology and their ability to induce an ex vivo IFN- γ response in PPD+ human peripheral blood mononuclear cells (PBMC), suggesting that they are immunogenic in humans [57,58]. ID91 antigens were cloned into an alphavirus repRNA backbone, as previously described [49] (Figure 1B). This repRNA platform has a number of advantages, including (1) a subgenomic promoter to amplify the expression of the antigen of interest, (2) exclusive cytoplasmic activity with no risks of nuclear genomic integration, and (3) sustained antigen production in the presence of adjuvating innate responses that allow for dose-sparing and strong cellular responses [49,50]. Using Western blotting, we observed the efficient expression of the ID91 antigens from repRNA ID91 in BHK cells (Figures 1C and S1), demonstrating that this platform is amenable to *M.tb* antigen expression. Partnering repRNA with delivery formulations provides stability and protection from RNAses and removes the requirement for viral delivery, eliminating anti-vector immunity, which has been detrimental for promising candidates.

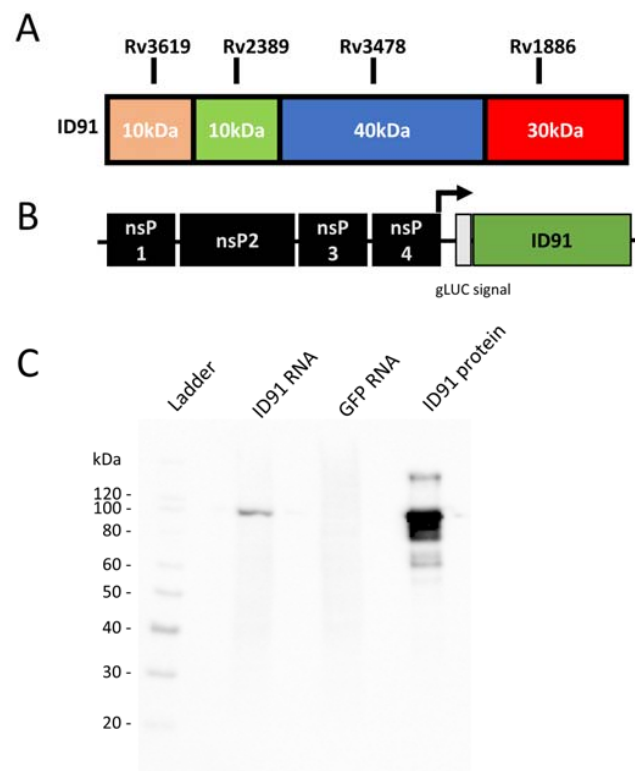


Figure 1. Design and Characterization of ID91 repRNA vaccine candidate. (A) ID91 fusion protein comprising 4 *M.tb* Antigens Rv3619, Rv2389, Rv3478, Rv1886. (B) Alphavirus backbone expressing nonstructural proteins (nsP) and ID91 fusion antigen. (C) Western blot of ID91 antigen expression from transfected BHK cell lysate in vitro after 24 h. From left to right: Ladder, Cell lysate from BHK transfected with ID91 RNA, GFP RNA, ID91 protein.

Here, we leveraged a first-generation nanostructured lipid carrier (NLC) [49] as a two-vial approach with ID91-repRNA. The C57BL/6 mice were vaccinated two times three weeks apart with either our existing next-generation ID91 fusion protein [57] +TLR4 agonist, glucopyranosyl lipid adjuvant formulated in a stable emulsion (GLA-SE) as a positive control for CD4⁺ T-cell responses and prophylactic efficacy against *M.tb* or a novel candidate ID91-repRNA + NLC to evaluate rep-RNA induced preliminary immunogenicity (Figure 2A). Splenocytes from both immunized groups were stimulated two weeks post-boost with media alone, ID91 protein or each of 13 different 15 mer peptide pools overlapping by 8 mers of ID91 and evaluated for proliferation and cytokine responses (Figure 2B, representative gating in Figure S2). We observed that ID91 + GLA-SE elicited both CD4⁺ (Red) and CD8⁺ (Blue) T-cell responses, albeit larger CD4⁺ TH1, while ID91-repRNA + NLC largely drove CD8⁺ T-cell proliferation and inflammatory cytokines (Figure 2B). For the ID91 protein/GLA-SE vaccine, we observed both CD4⁺ and CD8⁺ epitopes in the ID91 antigen fusion. Vaccination with ID91 + GLA-SE elicited measurably higher proliferative CD4⁺ T-cell responses from peptide pool numbers 2, 4, 10, 12, and 13, whereas pools 3, 4, 10, 11, and 12 induced measurable proliferation in the CD8⁺ T cell compartment (Figure 2B). Amino acid sequence LVAAAKMWDSVSDLFSAASAFQSVVWGL (peptides #33–35, pool 4) from Rv3478 may contain dominant epitopes for both CD4⁺ and CD8⁺ T cells. Unlike the protein-adjuvant strategy, repRNA ID91 + NLC induces measurable CD8⁺ but not CD4⁺ T-cell proliferation and cytokine induction upon restimulation of splenocytes *ex vivo*, with the most dominant epitopes in Rv1886 (Figure 2B, Table 1).

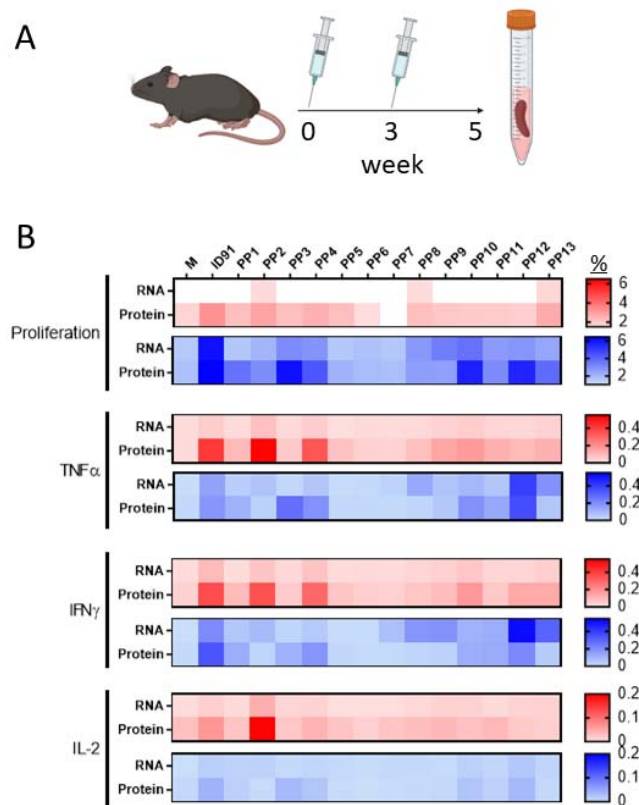


Figure 2. Epitope mapping of T-cell responses with different vaccine platforms. (A) Vaccination scheme. C57BL/6 mice were immunized twice, three weeks apart, with ID91 repRNA + NLC (RNA) or ID91 + GLA-SE. (B) Two weeks post-boost, splenocytes were stimulated with media (M) whole antigen (ID91) or 13 different peptide pools (PP) with overlapping 15 mers of ID91. Proliferation and cytokine expression were measured by flow cytometry after stimulation. Heat map depicts the percentage of CD4⁺ (red)- or CD8⁺ (blue)-responding T cells from each immunization depicted to the left (RNA or Protein). Data representative of a single experiment with $n = 4$ animals per group.

3.2. Immunogenicity and Prophylactic Protective Efficacy

We first evaluated ID91 repRNA and ID91-GLA-SE prophylactic immunizations in C57BL/6 mice for immunogenicity as well as protection from infection six weeks after a single immunization as a stringent criterion for advancing this platform (Figure 3A). A single vaccination with ID91 + GLA-SE induced robust CD4⁺ CD44⁺ TH1 T cells expressing IFN γ , IL-2, and TNF (Figure 3B), but negligible CD8⁺ CD44⁺ cytokine-producing T cells (Figures 3C and S3). Conversely, ID91 repRNA + NLC trended (but not significant) towards the higher induction of IFN γ , IL-2 or TNF-producing CD8⁺ CD44⁺ T cells (Figure 3C) as well as moderate generation of TH1 CD4⁺ T-cell responses (Figure 3B). No significant IL17a or IL-21 expression was observed for any group. Both of the vaccines induced a robust total IgG humoral immune response to the ID91 fusion, significantly greater than the saline group but not significantly different between the two platforms, with the bulk of this response being against antigen Rv1886 (Figure 3D). Lastly, we observed that both ID91 + GLA-SE and ID91 repRNA + NLC reduced lung bacterial burden, 0.55 and 0.43 log protection versus saline, respectively, three weeks post-challenge with a low-dose aerosol (LDA 50-100 colony-forming units [CFU]) of *M.tb* H37Rv (Figure 3E). These data demonstrate that the repRNA platform is immunogenic and affords some prophylactic protection in a stringent preclinical mouse efficacy screening model of TB.

Next, we evaluated the protein- and RNA-based platforms for immunogenicity and protection against an ultra-low dose (ULDA, 1–8 bacteria) of the H37Rv challenge using heterologous, homologous, and combination prime-boost strategies (Figure 4A). For the combination strategies, the mice were given both ID91 + GLA-SE and ID91 repRNA + NLC i.m. in separate limbs at prime and boost time points to avoid potential innate immune-mediated interference between the two modalities. We hypothesized that driving CD4⁺ and CD8⁺ T-cell responses may have an additive or synergistic effect on immunogenicity and provide subsequent protection from the more physiologically relevant ULDA challenge. We observed that two immunizations with ID91 + GLA-SE enhanced protection in the lung (0.743 log₁₀) over a single dose (Table 2, Figure 4B), which is in line with prior publications from our group [59]. However, two immunizations with ID91 repRNA + NLC only afforded a moderate reduction in bacterial burden in the lung, 0.306 log₁₀ (Table 2, Figure 4B), which we believe may be due to the suboptimal timing between the prime and boost vaccinations based on recent observations outside the scope of this manuscript. Heterologous strategies also differed, with RNA-prime protein-boost being the most efficacious regimen evaluated for reduced lung bacterial load (0.847 log₁₀ reduction), followed closely by the combination regimen (0.809 log₁₀ reduction) (Table 2, Figure 4B). While the combination regimen appears to be the most protective from dissemination to the spleen (1.419 log₁₀ reduction from saline), this was not statistically significant due to a wide standard error (Table 2, Figure 4C).

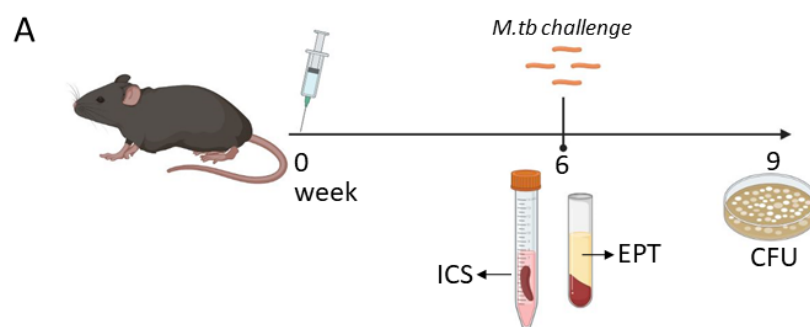


Figure 3. Cont.

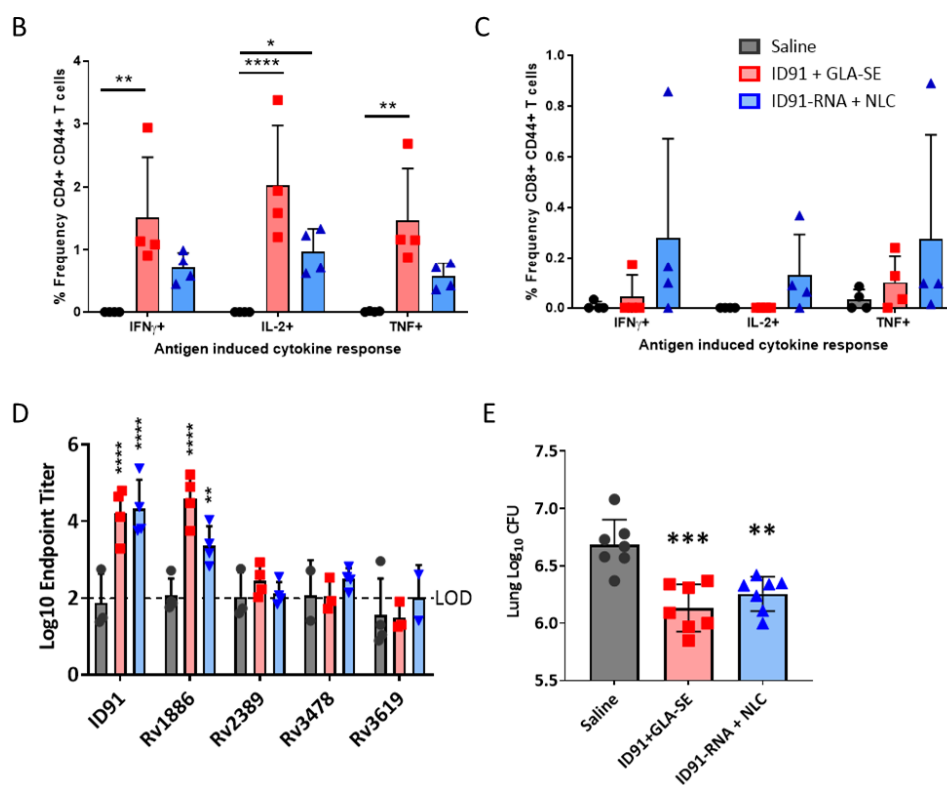


Figure 3. Single immunization with repRNA vaccine is moderately immunogenic and affords prophylactic protection. (A) Experimental schematic showing splenocytes from cohorts of saline (grey circles), ID91 + GLA-SE (red squares) or ID91 repRNA + NLC (blue triangles) immunized mice 6 weeks post-vaccination were stimulated with ID91 ex vivo and evaluated by intracellular cytokine staining flow cytometry including (B) percentage of CD4 + CD44 cytokine-producing T cells as well as (C) percentage of CD8+ CD44+ cytokine-producing T cells after medium subtraction. *n* = 4 per group. (D) Plasma was evaluated 6 weeks post-vaccination for total IgG responses to fusion antigen ID91 and its components, Log10 endpoint titer (EPT) is shown. *n* = 4 per group. (E) Pulmonary bacterial burden Log10 CFU 3 weeks post-LDA challenge with M.tb H37Rv. *n* = 7 per group, mean value and SEM shown with Y-axis beginning at 5.5 Log10 CFU. Asterisks represent a statistically significant difference from saline using One-way ANOVA with Dunnett’s multiple-comparison test. All data are representative of two independent repeated experiments. * *p* < 0.05, ** *p* < 0.01, *** *p* < 0.001 and **** *p* < 0.0001.

Table 2. Immunogenicity and Efficacy using Prime-Boost regimens.

| Candidate Regimen | | CFU Log10 ± SEM | | CFU Log10 Reduction [§] | | Log10 ID91 Total IgG EPT [§] | % ID91 CD4+ T cells [#] | % ID91 CD8+ T cells [#] |
|-------------------|----------------|-----------------|-------------|----------------------------------|-----------------------------|---------------------------------------|----------------------------------|----------------------------------|
| Prime | Boost | Lung | Spleen | Lung | Spleen | | | |
| Saline | Saline | 5.36 ± 0.09 | 4.08 ± 0.48 | - | - | 2.18 | 0.398 | 0.304 |
| ID91 + GLA-SE | ID91 + GLA-SE | 4.61 ± 0.15 | 3.52 ± 0.63 | 0.743 ** <i>p</i> = 0.0075 | 0.557 <i>p</i> = 0.9638 | 8.25 **** <i>p</i> < 0.0001 | 1.209 <i>p</i> = 0.3415 | 1.198 <i>p</i> = 0.8055 |
| ID91-RNA + NLC | ID91-RNA + NLC | 5.05 ± 0.017 | 4.51 ± 0.74 | 0.306 <i>p</i> = 0.4731 | -0.427 <i>p</i> = 0.9883 | 4.98 **** <i>p</i> < 0.0001 | 0.212 <i>p</i> = 0.9944 | 1.512 <i>p</i> = 0.9952 |
| ID91 + GLA-SE | ID91-RNA + NLC | 4.93 ± 0.11 | 4.58 ± 0.39 | 0.428 <i>p</i> = 0.1920 | -0.501 <i>p</i> = 0.9765 | 6.09 **** <i>p</i> < 0.0001 | 0.748 <i>p</i> = 0.9216 | 0.994 <i>p</i> = 0.9573 |
| ID91-RNA + NLC | ID91 + GLA-SE | 4.51 ± 0.18 | 3.72 ± 0.57 | 0.847 ** <i>p</i> = 0.0021 | 0.358 <i>p</i> = 0.9947 | 6.87 **** <i>p</i> < 0.0001 | 1.088 <i>p</i> = 0.4890 | 1.110 <i>p</i> = 0.9945 |
| Combination | Combination | 4.54 ± 0.13 | 2.66 ± 0.76 | 0.809 ** <i>p</i> = 0.0047 | 1.419 <i>p</i> = 0.4273 | 7.45 **** <i>p</i> < 0.0001 | 1.711 * <i>p</i> = 0.0487 | 3.048 * <i>p</i> = 0.0226 |

[§] Vaccine cohort mean values compared to the saline group; significance evaluated by using One-way ANOVA with Dunnett’s multiple-comparison test denoted by asterisk. CFU standard error for lung = 0.219, spleen = 0.938. [#] Magnitude of Polyfunctional T-cell responses include IFN γ , TNF and IL-2 cytokines in % ID91-specific T-cell responses. Data representative of two independent repeat studies for CFU, and EPT, data representative of one repeat for T cell data. *n* = 7–6/group for CFU, *n* = 4/group for EPT and T cell evaluations. * *p* < 0.05, ** *p* < 0.01 and **** *p* < 0.0001.

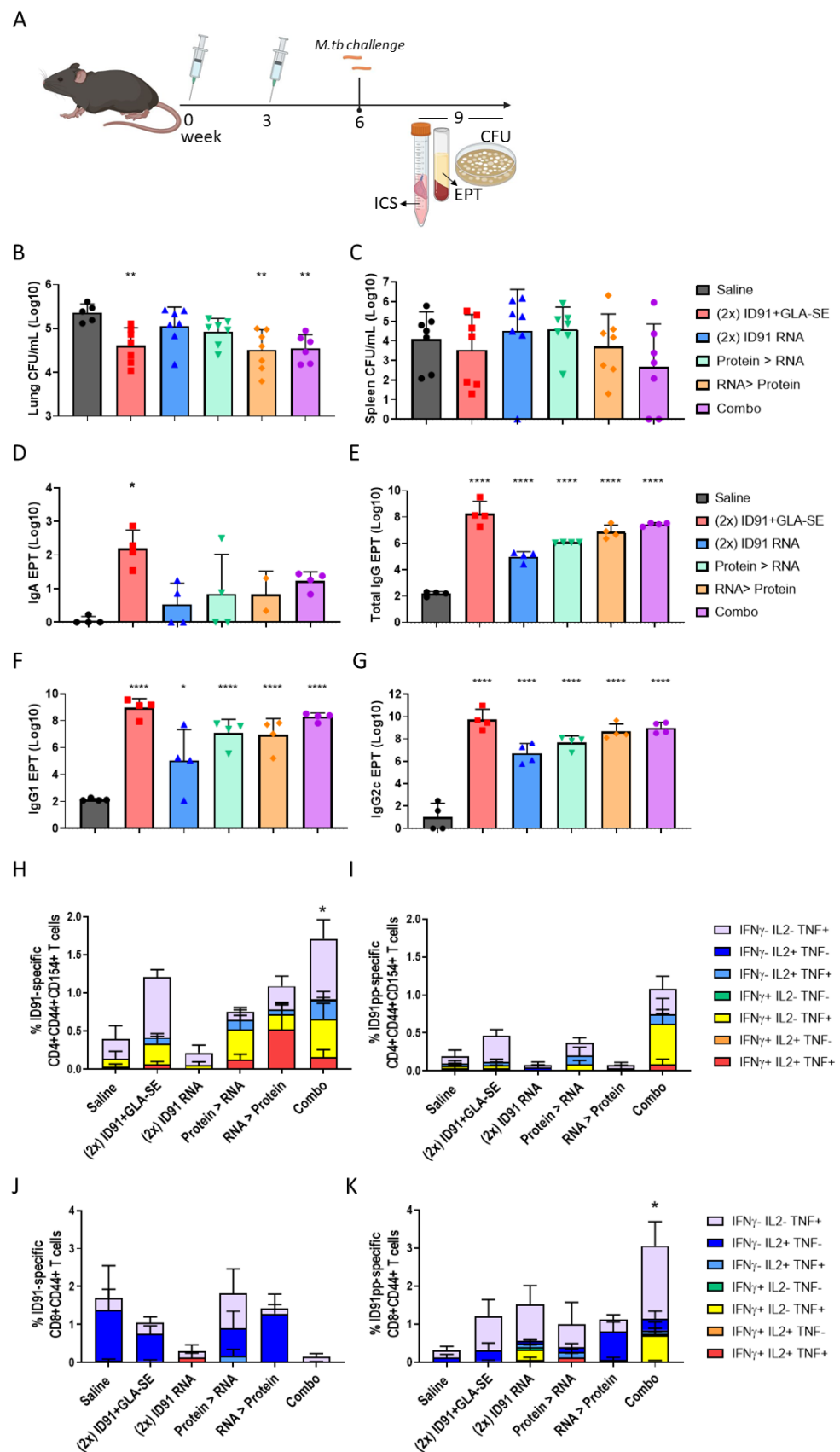


Figure 4. Regimen composition influences protection and post-challenge immune responses. (A) vaccination and sample schematic. Bacterial burden assessed by colony-forming units (CFU) in (B) the lung and (C) spleen homogenates 3 weeks post-challenge. *n* = 6–7 mice per cohort, saline–grey,

homologous ID91 + GLA-SE-red, homologous ID91 repRNA +NLC-blue, protein prime/RNA boost-green, RNA prime/protein boost-orange, and combination-purple. Y-axis for (B) does not begin at zero. (D) BALf from $n = 4$ mice per cohort was collected 3 weeks post-challenge and evaluated for ID91-specific IgA responses. Plasma from $n = 4$ mice per cohort was isolated 3 weeks post-challenge and evaluated for ID91-specific (E) Total IgG, (F) IgG1 and (G) IgG2c. CFU and EPT group means were compared to saline by ordinary One-Way ANOVA and Dunnet's multiple comparisons test. Single-cell suspensions isolated from the lungs of animals 3 weeks post-ULDA challenge were stimulated with ID91 protein (H,J) or ID91 peptide pool (I,K) and evaluated for (H,I) CD4+ CD44+ CD154+ and (J,K) CD8+ CD44+ T cell expression of IFN γ , IL-2 and TNF by flow cytometry. $n = 4$ per group. All data are representative of two independent repeated experiments. Cytokine expression was compared using a One-Way ANOVA and Dunnet's multiple comparisons test. * $p < 0.05$, ** $p < 0.01$ and **** $p < 0.0001$.

This pattern of efficacy is largely mirrored in the post-challenge humoral and cellular immunogenicity readouts. While i.m. vaccine strategies are not known for developing robust mucosal immune responses, we evaluated bronchoalveolar lavage fluid for anti-ID91 IgA responses at 3 weeks post-challenge. Not surprisingly, the magnitude of IgA produced by all regimens was low, and homologous ID91 + GLA-SE was the only strategy to induce a statistically significant response compared to saline (Figure 4D). We observed that the combination and homologous ID91 + GLA-SE regimens induced the highest ID91-specific total IgG endpoint titers in serum (EPT) post-challenge, 7.45 log $_{10}$ and 8.25 log $_{10}$, respectively (Table 2, Figure 4E). They are followed by heterologous regimens, while the lowest total IgG induced was in the homologous RNA cohort (Table 2, Figure 4E). Similar trends were observed for ID91-specific IgG1 (Figure 4F) and IgG2c (Figure 4G), with homologous protein and combination regimens demonstrating the highest EPT and homologous RNA the lowest EPT.

Interestingly we did not observe significant differences in the ID91-specific stimulation of the individual cytokines IL-2, GM-CSF, or IL-17A from CD4+ nor CD8+ T cells between the treatment groups. However, CD4+ T cell TNF expression was statistically higher in the heterologous RNA prime, protein boost, and combination regimens, and CD8+ T cell TNF expression was significantly higher in the combination regimen. Given the relative paucity of strong CD8+ epitopes in ID91 antigens, it was not a surprise to observe the expression of CD107a on CD8+ CD44+ T cells post-challenge to be statistically similar between the cohorts. We also examined polyfunctional CD4+ and CD8+ T-cell responses by using flow cytometry results from each cohort after the ex vivo stimulation of the lung cells and found that only the combination regimen induced a significantly higher total magnitude of responses for both the CD4+ and CD8+ subsets (Figure 4H–K, Table 2, representative gating Figure S4). We observed the greatest magnitude and diversity of responses for CD4+ T cells in the context of protein stimulation and for CD8+ T cells in the context of peptide pool stimulation. While not significant, there is a trend for the most robust polyfunctional CD4+ T-cell responses in regimens that include at least one arm, including protein immunizations. We observed the composition of polyfunctional cells to be relatively similar (Figure 4H–K). Triple-positive (IFN γ , IL-2, and TNF), dual-expressing IFN γ + TNF+, and single-TNF-positive cells made up the majority of the CD4+ T-cell responses across the regimens evaluated, with either protein or peptide stimulations. While single-positive IL-2+ or TNF+ responses overwhelmingly dominated the CD8+ T-cell response in this post-challenge ex vivo stimulation with either protein or peptide pools (Figure 4H–K). The homologous RNA group and combination groups seem to have the most diverse CD8+ T-cell responses when restimulated with peptide pools, but these are largely lost in the context of full-protein stimulation (Figure 4J,K).

4. Discussion

These data provide the first report of a replicating RNA-based vaccine strategy being evaluated in the M.tb mouse challenge model and showing efficacy in heterologous and combination regimens. While ID91 served here as a proof-of-concept antigen that afforded some protection from the bacterial burden, epitope mapping demonstrated that ID91 contains few dominant CD8+ T-cell epitopes in the C57BL/6 mouse model and is, therefore, not a high-priority candidate for the repRNA platform. Future work that incorporates antigens containing CD8+ T-cell epitopes [30,60,61] should be prioritized and include specific mechanistic studies that evaluate the contribution of CD8+ T cells elicited by the RNA platform. The ability to readily swap antigens lends itself well to the needs of TB vaccines since global regions harbor different predominant lineages [62], and tailoring vaccines to meet regional needs may further help improve efficacy. Indeed, while we observed modest protection from bacterial burden in the lungs of homologous protein and heterologous candidate vaccinated mice, there was an absence of protection observed in the spleen at this timepoint evaluated. Improving protection from dissemination should be an additional selection criterion for novel antigen selection.

While there is some overlap in the CD4+ and CD8+ responses driven by each immunization strategy, these data demonstrate that RNA and protein differentially elicit CD4+ and CD8+ T-cellular responses to distinct antigen epitopes (Figure 2B), which may be beneficial for heterologous vaccine approaches. This is congruent with clinical trials of a similar but more advanced clinical vaccine candidate, ID93 + GLA-SE, where we have observed protein-adjuvant vaccine-elicited immunogenicity to be dominated by CD4+ TH1 responses and far fewer cases (four responders of 38 across all of the regimens tested, ClinicalTrials.gov number NCT02465216) demonstrating CD8+ T-cell-based responses [63].

We observed that the heterologous and combination regimens were moderately additive in reducing pulmonary bacterial burden in this preclinical model. Importantly we observed that the repRNA platform induced immunogenic responses to ID91 antigens both post-vaccine boost as well as the post-M.tb challenge. These were measured by robust systemic antigen-specific antibody responses and some evidence of mucosal-driven immunity with the detection of ID91-specific IgA in the BALf of the immunized animals compared to the saline mouse cohorts. We also note that the cellular CD4+ and CD8+ T-cell responses were differentially induced by each platform, and the polyfunctional responses were disparate depending on the regimen being evaluated in the post-challenge time point. Those regimens containing a repRNA arm did display enhanced magnitude or composition of polyfunctional responses post-challenge than saline or protein-only controls. These data suggest that the repRNA vaccine is eliciting a measurably broader CD8+ T-cell response, even in the condition of an antigen with few epitopes.

It is interesting that the heterologous protein > repRNA cohorts and repRNA > protein cohorts did not behave similarly in the protection or immunogenicity readouts. In fact, we observed that the repRNA > protein regimens were more protective (lung bacterial burden) and induced more polyfunctional CD4+ T cells than protein > RNA regimens, albeit these differences were small. We speculate this may have to do with the repRNA > protein regimen allowing for the establishment of CD8+ T-cell responses in tandem with CD4+ responses instead of a dominating CD4+ response that takes over at the expense of resources for the CD8+ T cells. More work to define these properties and establish this mechanism is needed. While no single immunological endpoint (total IgG, IgG1, IgG2c, IgA EPT, TH1 CD4+ or CD8+ T cells) correlated with protective efficacy, there are interesting trends that may be further explored and optimized. Indeed, our data suggest that meeting the thresholds for specific combinations of responses versus single endpoints may better correlate with protective efficacy in this model.

5. Conclusions

The landscape of TB vaccines is ready for a dramatic surge forward. A key advantage of RNA platforms is their ability to stimulate antigen-specific CD8+ T cells and antibody

responses, which both aid in the control of intracellular infections. As a result, heterologous and co-immunization strategies that combine protein and nucleic acid vaccines are promising approaches for inducing protective immunity through CD4+ and CD8+ T cell-mediated responses [64,65]. In our observations, we also saw that polyfunctional CD4+ T-cell responses were generated in the heterologous regimens, so the inclusion of repRNA will not be to the detriment of this important cell type for TB control.

Future interrogations should examine other immune correlates that are showing promise, including IgM, as well as the localization and kinetics of CD4+ and CD8+ T-cell responses [44,66]. The mucosal or aerosol delivery of repRNA in specialized delivery formulations may also help drive pulmonary-specific immunity against *M.tb*, and these strategies are currently being evaluated. Research outside the scope of this work is currently ongoing to formulate repRNA for aerosol or i.n. delivery. We hypothesize that leveraging repRNA in a heterologous prime-pull technique may provide the balance of durable systemic and mucosal immunity, which is showing promise in recent preclinical models as correlates of protection [44]. Our prior work with protein+ adjuvant candidates has shown that intranasal administration retains protective efficacy in the mouse model and enhances the induction of tissue-resident TH17 cells [67], which also may contribute to TB control. The optimal heterologous regimen composition, route, and regimen are outside the scope of this study, but they are ongoing questions in our laboratories.

Evaluating alternative repRNA expression strategies and alternative timing between prime and boost immunizations can be explored to optimize B- and T-cell responses against antigens of interest. For example, here we evaluated a prime/boost spaced 3 weeks apart in our ULDA challenge and have more recently established that 4–8 weeks between prime and boost drives better immune responses in regimens that include the repRNA platform (unpublished and [50]). We believe that the moderate additive effect seen here with the heterologous and combination regimens, compared to the LDA study with a 6-week rest before the challenge, could be significantly improved by increasing the vaccine interval timing. Here, we examined LDA and ULDA challenges with laboratory-adapted *M.tb* H37Rv; follow-on work should evaluate the efficacy against clinical isolates representing major *M.tb* lineages.

While this preclinical proof of concept work leveraged an NLC formulation, next-generation RNA vaccine formulations have advanced into clinical trials (e.g., HDT BioCorp: state-of-the-art delivery vehicle Lipid InOrganic Nanoparticle (LION) [50], US ClinicalTrials.gov Identifier: NCT04844268, India CTRI/2021/04/032688) and the development of RNA-based *M.tb* vaccines should engage these formulations or others [68–72] with proven human safety data to help accelerate this platform and address the ongoing TB epidemic. In summary, the repRNA platform shows promise as an immunogenic vaccine strategy for TB, and a well-designed set of *M.tb* antigens in partnership with advanced RNA formulations have the capability to significantly contribute to the TB vaccine pipeline.

Supplementary Materials: The following supporting information can be downloaded at: <https://www.mdpi.com/article/10.3390/vaccines11010130/s1>, Figure S1: Uncropped Western Blots using-ID91 polyclonal sera. Cropped blot image referenced in Figure 1; Figure S2: Representative Gating for Epitope Mapping; Figure S3: Representative Gating for Pre-challenge Immunogenicity; Figure S4: Representative Gating for post-challenge Immunogenicity.

Author Contributions: Conceptualization, S.E.L., S.L.B. and R.N.C.; methodology, S.E.L., J.H.E., S.L.B. and R.N.C.; formal analysis, S.E.L., V.A.R. and T.P.; investigation, S.E.L., J.H.E., V.A.R., T.P., J.A., A.K., F.-C.H. and K.N.; resources, J.H.E. and A.K.; data curation, S.E.L., F.-C.H., V.A.R. and T.P.; writing—S.E.L.; writing—review and editing, S.E.L., J.H.E., V.A.R., T.P., J.A., A.K., F.-C.H., S.G.R., S.L.B. and R.N.C.; visualization, S.E.L., T.P. and V.A.R.; supervision, S.L.B. and R.N.C.; funding acquisition, S.E.L., S.L.B. and R.N.C. All authors have read and agreed to the published version of the manuscript.

Funding: Research reported here was supported by the National Institute of Allergy and Infectious Diseases (NIAID) of the National Institutes of Health (NIH) under award number R01AI125160. This work was also supported by the GCRF Networks in Vaccines Research and Development VALIDATE Network, which was co-funded by the MRC and BBSRC (ref MR/R005850/1). This UK-funded award is part of the EDCTP2 programme supported by the European Union. SEL was supported through the University of Washington, Diseases of Public Health Importance training grant number T32A1075090. The content is solely the responsibility of the authors and does not necessarily represent the official views of the National Institutes of Health, MRC or BBSRC.

Institutional Review Board Statement: The animal study protocol was approved by the Institutional Animal Care and Use Committee (IACUC) of the Institute formerly known as the Infectious Disease Research Institute (IDRI) (protocol number 2017-9, approved 9 March 2017) which operated under USDA Certificate # 91-R-0061 and PHS Assurance # A4337-01.

Informed Consent Statement: Not applicable.

Data Availability Statement: Data are reported in the manuscript or can be made available upon request from the authors.

Acknowledgments: The authors would like to express their gratitude to Seattle Children's Research Institute Leadership for their guidance, compassion, and mentorship. Schematic images created with Biorender.com. The authors would also like to thank Zhiyi Zhu (Seattle Children's Research Institute) for his help during the review process and collegiality.

Conflicts of Interest: The authors declare no conflict of interest. The funders had no role in the design of the study; in the collection, analyses, or interpretation of data; in the writing of the manuscript; or in the decision to publish the results.

References

1. World Health Organization. *Global Tuberculosis Report*; World Health Organization: Geneva, Switzerland, 2019.
2. World Health Organization. *Global Tuberculosis Report 2020: Executive Summary*; World Health Organization: Geneva, Switzerland, 2020.
3. World Health Organization. *Global Tuberculosis Report*; World Health Organization: Geneva, Switzerland, 2021.
4. Cucinotta, D.; Vanelli, M. WHO Declares COVID-19 a Pandemic. *Acta Biomed.* **2020**, *91*, 157–160. [[CrossRef](#)]
5. World Health Organization. *Global Tuberculosis Report 2018*; World Health Organization: Geneva, Switzerland, 2018.
6. World Health Organization. *Global TB Report*; World Health Organization: Geneva, Switzerland, 2022.
7. World Health Organization Global TB Programme. *Impact of the COVID-19 Pandemic on TB Detection and Mortality in 2020*; World Health Organization: Geneva, Switzerland, 2021.
8. Zaman, K. Tuberculosis: A global health problem. *J. Health Popul. Nutr.* **2010**, *28*, 111–113. [[CrossRef](#)]
9. Mallapaty, S.; Callaway, E.; Kozlov, M.; Ledford, H.; Pickrell, J.; Van Noorden, R. How COVID vaccines shaped 2021 in eight powerful charts. *Nature* **2021**, *600*, 580–583. [[CrossRef](#)]
10. Parveen, U.; Sultana, S.; Heba, S.F.; Rafi, R.; Begum, A.; Fatima, N. Pretomanid: A novel therapeutic paradigm for treatment of drug resistant tuberculosis. *Indian J. Tuberc.* **2021**, *68*, 106–113. [[CrossRef](#)]
11. Haldar, R.; Narayanan, S.J. A novel ensemble based recommendation approach using network based analysis for identification of effective drugs for Tuberculosis. *Math. Biosci. Eng.* **2022**, *19*, 873–891. [[CrossRef](#)] [[PubMed](#)]
12. Ahmed, S.; Nandi, S.; Saxena, A.K. An updated patent review on drugs for the treatment of tuberculosis (2018–present). *Expert Opin. Ther. Pat.* **2022**, *32*, 401–421. [[CrossRef](#)] [[PubMed](#)]
13. Almeida, D.; Converse, P.J.; Li, S.-Y.; Upton, A.M.; Fotouhi, N.; Nuermberger, E.L. Comparative Efficacy of the Novel Diarylquinoline TBAJ-876 and Bedaquiline against a Resistant Rv0678 Mutant in a Mouse Model of Tuberculosis. *Antimicrob. Agents Chemother.* **2021**, *65*, e0141221. [[CrossRef](#)]
14. Larkins-Ford, J.; Greenstein, T.; Van, N.; Degefu, Y.N.; Olson, M.C.; Sokolov, A.; Aldridge, B.B. Systematic measurement of combination-drug landscapes to predict in vivo treatment outcomes for tuberculosis. *Cell Syst.* **2021**, *12*, 1046–1063.e1047. [[CrossRef](#)]
15. Houben, R.M.G.J.; A Menzies, N.; Sumner, T.; Huynh, G.H.; Arinaminpathy, N.; Goldhaber-Fiebert, J.D.; Lin, H.-H.; Wu, C.-Y.; Mandal, S.; Pandey, S.; et al. Feasibility of achieving the 2025 WHO global tuberculosis targets in South Africa, China, and India: A combined analysis of 11 mathematical models. *Lancet Glob. Health* **2016**, *4*, e806–e815. [[CrossRef](#)] [[PubMed](#)]
16. Menzies, N.; Gomez, G.B.; Bozzani, F.; Chatterjee, S.; Foster, N.; Baena, I.G.; Laurence, Y.V.; Qiang, S.; Siroka, A.; Sweeney, S.; et al. Cost-effectiveness and resource implications of aggressive action on tuberculosis in China, India, and South Africa: A combined analysis of nine models. *Lancet Glob. Health* **2016**, *4*, e816–e826. [[CrossRef](#)] [[PubMed](#)]

17. Arregui, S.; Iglesias, M.J.; Samper, S.; Marinova, D.; Martin, C.; Sanz, J.; Moreno, Y. Data-driven model for the assessment of Mycobacterium tuberculosis transmission in evolving demographic structures. *Proc. Natl. Acad. Sci. USA* **2018**, *115*, E3238–E3245. [[CrossRef](#)]
18. Roy, A.; Eisenhut, M.; Harris, R.J.; Rodrigues, L.C.; Sridhar, S.; Habermann, S.; Snell, L.B.; Mangtani, P.; Adetifa, I.; Lalvani, A.; et al. Effect of BCG vaccination against Mycobacterium tuberculosis infection in children: Systematic review and meta-analysis. *BMJ* **2014**, *349*, g4643. [[CrossRef](#)] [[PubMed](#)]
19. Van Der Meeren, O.; Hatherill, M.; Nduba, V.; Wilkinson, R.J.; Muyoyeta, M.; Van Brakel, E.; Ayles, H.M.; Henostroza, G.; Thienemann, F.; Scriba, T.J.; et al. Phase 2b Controlled Trial of M72/AS01(E) Vaccine to Prevent Tuberculosis. *N. Engl. J. Med.* **2018**, *379*, 1621–1634. [[CrossRef](#)]
20. Tait, D.R.; Hatherill, M.; Van Der Meeren, O.; Ginsberg, A.M.; Van Brakel, E.; Salaun, B.; Scriba, T.J.; Akite, E.J.; Ayles, H.M.; Bollaerts, A.; et al. Final Analysis of a Trial of M72/AS01E Vaccine to Prevent Tuberculosis. *N. Engl. J. Med.* **2019**, *381*, 2429–2439. [[CrossRef](#)] [[PubMed](#)]
21. Martin, C.; Aguilo, N.; Marinova, D.; Gonzalo-Asensio, J. Update on TB Vaccine Pipeline. *Appl. Sci.* **2020**, *10*, 2632. [[CrossRef](#)]
22. Lewinsohn, D.A.; Lewinsohn, D.M.; Scriba, T.J. Polyfunctional CD4(+) T Cells as Targets for Tuberculosis Vaccination. *Front. Immunol.* **2017**, *8*, 1262. [[CrossRef](#)]
23. Tameris, M.D.; Hatherill, M.; Landry, B.S.; Scriba, T.J.; Snowden, M.A.; Lockhart, S.; E Shea, J.; McClain, J.B.; Hussey, G.D.; A Hanekom, W.; et al. Safety and efficacy of MVA85A, a new tuberculosis vaccine, in infants previously vaccinated with BCG: A randomised, placebo-controlled phase 2b trial. *Lancet* **2013**, *381*, 1021–1028. [[CrossRef](#)]
24. Lu, L.L.; Smith, M.T.; Yu, K.K.Q.; Luedemann, C.; Suscovich, T.J.; Grace, P.S.; Cain, A.; Yu, W.H.; McKittrick, T.R.; Lauffenburger, D.; et al. IFN- γ -independent immune markers of Mycobacterium tuberculosis exposure. *Nat. Med.* **2019**, *25*, 977–987. [[CrossRef](#)]
25. Smith, C.M.; Proulx, M.K.; Lai, R.; Kiritsy, M.C.; Bell, T.A.; Hock, P.; de Villena, F.P.-M.; Ferris, M.T.; Baker, R.E.; Behar, S.M.; et al. Functionally Overlapping Variants Control Tuberculosis Susceptibility in Collaborative Cross Mice. *mBio* **2019**, *10*, e02791-19. [[CrossRef](#)]
26. Behar, S.M. Antigen-specific CD8(+) T cells and protective immunity to tuberculosis. *Adv. Exp. Med. Biol.* **2013**, *783*, 141–163. [[CrossRef](#)]
27. Behar, S.M.; Woodworth, J.S.; Wu, Y. Next generation: Tuberculosis vaccines that elicit protective CD8+ T cells. *Expert Rev. Vaccines* **2007**, *6*, 441–456. [[CrossRef](#)] [[PubMed](#)]
28. Boom, W.H. New TB vaccines: Is there a requirement for CD8 T cells? *J. Clin. Investig.* **2007**, *117*, 2092–2094. [[CrossRef](#)]
29. Lazarevic, V.; Flynn, J. CD8+ T cells in tuberculosis. *Am. J. Respir. Crit. Care Med.* **2002**, *166*, 1116–1121. [[CrossRef](#)] [[PubMed](#)]
30. Lewinsohn, D.A.; Swarbrick, G.M.; Park, B.; Cansler, M.E.; Null, M.D.; Toren, K.G.; Baseke, J.; Zalwango, S.; Mayanja-Kizza, H.; Malone, L.L.; et al. Comprehensive definition of human immunodominant CD8 antigens in tuberculosis. *Npj. Vaccines* **2017**, *2*, 8. [[CrossRef](#)] [[PubMed](#)]
31. Lin, P.L.; Flynn, J.L. CD8 T cells and Mycobacterium tuberculosis infection. *Semin. Immunopathol.* **2015**, *37*, 239–249. [[CrossRef](#)]
32. Kamath, A.B.; Woodworth, J.; Xiong, X.; Taylor, C.; Weng, Y.; Behar, S.M. Cytolytic CD8+ T cells recognizing CFP10 are recruited to the lung after Mycobacterium tuberculosis infection. *J. Exp. Med.* **2004**, *200*, 1479–1489. [[CrossRef](#)]
33. Jeyanathan, M.; Mu, J.; McCormick, S.; Damjanovic, D.; Small, C.-L.; Shaler, C.R.; Kugathasan, K.; Xing, Z. Murine airway luminal antituberculous memory CD8 T cells by mucosal immunization are maintained via antigen-driven in situ proliferation, independent of peripheral T cell recruitment. *Am. J. Respir. Crit. Care Med.* **2010**, *181*, 862–872. [[CrossRef](#)] [[PubMed](#)]
34. Smith, S.M.; Klein, M.R.; Malin, A.S.; Sillah, J.; Huygen, P.; Andersen, P.; McAdam, K.P.W.J.; Dockrell, H.M. Human CD8(+) T cells specific for Mycobacterium tuberculosis secreted antigens in tuberculosis patients and healthy BCG-vaccinated controls in The Gambia. *Infect. Immun.* **2000**, *68*, 7144–7148. [[CrossRef](#)]
35. Tascon, R.E.; Stavropoulos, E.; Lukacs, K.V.; Colston, M.J. Protection against Mycobacterium tuberculosis infection by CD8+ T cells requires the production of gamma interferon. *Infect. Immun.* **1998**, *66*, 830–834. [[CrossRef](#)]
36. Müller, I.; Cobbold, S.P.; Waldmann, H.; Kaufmann, S.H. Impaired resistance to Mycobacterium tuberculosis infection after selective in vivo depletion of L3T4+ and Lyt-2+ T cells. *Infect. Immun.* **1987**, *55*, 2037–2041. [[CrossRef](#)] [[PubMed](#)]
37. Orme, I.M.; Collins, F.M. Adoptive protection of the Mycobacterium tuberculosis-infected lung. Dissociation between cells that passively transfer protective immunity and those that transfer delayed-type hypersensitivity to tuberculin. *Cell. Immunol.* **1984**, *84*, 113–120. [[CrossRef](#)]
38. Flynn, J.L.; Chan, J. Immunology of tuberculosis. *Annu. Rev. Immunol.* **2001**, *19*, 93–129. [[CrossRef](#)] [[PubMed](#)]
39. Cho, S.; Mehra, V.; Thoma-Uszynski, S.; Stenger, S.; Serbina, N.; Mazzaccaro, R.J.; Flynn, J.L.; Barnes, P.F.; Southwood, S.; Celis, E.; et al. Antimicrobial activity of MHC class I-restricted CD8+ T cells in human tuberculosis. *Proc. Natl. Acad. Sci. USA* **2000**, *97*, 12210–12215. [[CrossRef](#)] [[PubMed](#)]
40. Serbina, N.V.; Liu, C.C.; Scanga, C.A.; Flynn, J.L. CD8+ CTL from lungs of Mycobacterium tuberculosis-infected mice express perforin in vivo and lyse infected macrophages. *J. Immunol.* **2000**, *165*, 353–363. [[CrossRef](#)] [[PubMed](#)]
41. Serbina, N.V.; Flynn, J.L. CD8(+) T cells participate in the memory immune response to Mycobacterium tuberculosis. *Infect. Immun.* **2001**, *69*, 4320–4328. [[CrossRef](#)]

42. Brookes, R.H.; Pathan, A.A.; McShane, H.; Hensmann, M.; Price, D.A.; Hill, A.V.S. CD8+ T cell-mediated suppression of intracellular Mycobacterium tuberculosis growth in activated human macrophages. *Eur. J. Immunol.* **2003**, *33*, 3293–3302. [[CrossRef](#)] [[PubMed](#)]
43. Wang, J.; Thorson, L.; Stokes, R.W.; Santosuosso, M.; Huygen, K.; Zganiacz, A.; Hitt, M.; Xing, Z. Single mucosal, but not parenteral, immunization with recombinant adenoviral-based vaccine provides potent protection from pulmonary tuberculosis. *J. Immunol.* **2004**, *173*, 6357–6365. [[CrossRef](#)]
44. Darrah, P.A.; Zeppa, J.J.; Maiello, P.; Hackney, J.A.; Li, M.H.W.; Hughes, T.K.; Pokkali, S.; Li, P.A.S.; Grant, N.L.; Rodgers, M.A.; et al. Prevention of tuberculosis in macaques after intravenous BCG immunization. *Nature* **2020**, *577*, 95–102. [[CrossRef](#)] [[PubMed](#)]
45. Roordink, D.; Williams, A.; Fritzell, B.; Laddy, D.J.; Gerdil, E.; Graffin, A.M.; Tait, D.; van der Pol, L.; van den Brink, I.; Holleman, M.; et al. The TB vaccine development pathway—An innovative approach to accelerating global TB vaccine development. *Tuberculosis* **2021**, *126*, 102040. [[CrossRef](#)]
46. Whitlow, E.; Mustafa, A.S.; Hanif, S.N.M. An Overview of the Development of New Vaccines for Tuberculosis. *Vaccines* **2020**, *8*, 586. [[CrossRef](#)]
47. Verbeke, R.; Lentacker, I.; De Smedt, S.C.; Dewitte, H. The dawn of mRNA vaccines: The COVID-19 case. *J. Control. Release* **2021**, *333*, 511–520. [[CrossRef](#)]
48. Xue, T.; Stavropoulos, E.; Yang, M.; Ragno, S.; Vordermeier, M.; Chambers, M.; Hewinson, G.; Lowrie, D.B.; Colston, M.J.; Tascon, R.E. RNA encoding the MPT83 antigen induces protective immune responses against Mycobacterium tuberculosis infection. *Infect. Immun.* **2004**, *72*, 6324–6329. [[CrossRef](#)]
49. Erasmus, J.H.; Khandhar, A.P.; Guderian, J.; Granger, B.; Archer, J.; Archer, M.; Gage, E.; Fuerte-Stone, J.; Larson, E.; Lin, S.; et al. A Nanostructured Lipid Carrier for Delivery of a Replicating Viral RNA Provides Single, Low-Dose Protection against Zika. *Mol. Ther.* **2018**, *26*, 2507–2522. [[CrossRef](#)]
50. Erasmus, J.H.; Khandhar, A.P.; O'Connor, M.A.; Walls, A.C.; Hemann, E.A.; Murapa, P.; Archer, J.; Leventhal, S.; Fuller, J.T.; Lewis, T.B.; et al. An Alphavirus-derived replicon RNA vaccine induces SARS-CoV-2 neutralizing antibody and T cell responses in mice and nonhuman primates. *Sci. Transl. Med.* **2020**, *12*, eabc9396. [[CrossRef](#)]
51. Ljungberg, K.; Liljeström, P. Self-replicating alphavirus RNA vaccines. *Expert Rev. Vaccines* **2015**, *14*, 177–194. [[CrossRef](#)] [[PubMed](#)]
52. Leitner, W.W.; Hwang, L.N.; Deveer, M.J.; Zhou, A.; Silverman, R.H.; Williams, B.; Dubensky, T.W.; Ying, H.; Restifo, N.P. Alphavirus-based DNA vaccine breaks immunological tolerance by activating innate antiviral pathways. *Nat. Med.* **2003**, *9*, 33–39. [[CrossRef](#)]
53. Bertholet, S.; Ireton, G.C.; Ordway, D.J.; Windish, H.P.; Pine, S.O.; Kahn, M.; Phan, T.; Orme, I.M.; Vedvick, T.S.; Baldwin, S.L.; et al. A defined tuberculosis vaccine candidate boosts BCG and protects against multidrug-resistant Mycobacterium tuberculosis. *Sci. Transl. Med.* **2010**, *2*, 53ra74. [[CrossRef](#)] [[PubMed](#)]
54. Larsen, S.E.; Baldwin, S.L.; Orr, M.T.; Reese, V.A.; Pecor, T.; Granger, B.; Cauwelaert, N.D.; Podell, B.K.; Coler, R.N. Enhanced Anti-Mycobacterium tuberculosis Immunity over Time with Combined Drug and Immunotherapy Treatment. *Vaccines* **2018**, *6*, 30. [[CrossRef](#)] [[PubMed](#)]
55. Coler, R.N.; Bertholet, S.; Moutaftsi, M.; Guderian, J.A.; Windish, H.P.; Baldwin, S.L.; Laughlin, E.M.; Duthie, M.; Fox, C.; Carter, D.; et al. Development and characterization of synthetic glucopyranosyl lipid adjuvant system as a vaccine adjuvant. *PLoS ONE* **2011**, *6*, e16333. [[CrossRef](#)] [[PubMed](#)]
56. Larsen, S.E.; Reese, V.A.; Pecor, T.; Berube, B.J.; Cooper, S.K.; Brewer, G.; Ordway, D.; Henao-Tamayo, M.; Podell, B.K.; Baldwin, S.L.; et al. Subunit vaccine protects against a clinical isolate of Mycobacterium avium in wild type and immunocompromised mouse models. *Sci. Rep.* **2021**, *11*, 9040. [[CrossRef](#)] [[PubMed](#)]
57. Orr, M.T.; Ireton, G.C.; Beebe, E.A.; Huang, P.-W.D.; Reese, V.A.; Argilla, D.; Coler, R.N.; Reed, S.G. Immune subdominant antigens as vaccine candidates against Mycobacterium tuberculosis. *J. Immunol.* **2014**, *193*, 2911–2918. [[CrossRef](#)]
58. Bertholet, S.; Ireton, G.C.; Kahn, M.; Guderian, J.; Mohamath, R.; Stride, N.; Laughlin, E.M.; Baldwin, S.L.; Vedvick, T.S.; Coler, R.N.; et al. Identification of human T cell antigens for the development of vaccines against Mycobacterium tuberculosis. *J. Immunol.* **2008**, *181*, 7948–7957. [[CrossRef](#)]
59. Orr, M.T.; Ireton, G.C.; Beebe, E.A.; Huang, P.-W.D.; Reese, V.A.; Argilla, D.; Coler, R.N.; Reed, S.G. Elimination of the cold-chain dependence of a nanoemulsion adjuvanted vaccine against tuberculosis by lyophilization. *J. Control. Release* **2014**, *177*, 20–26. [[CrossRef](#)]
60. Tian, Y.; da Silva Antunes, R.; Sidney, J.; Lindestam Arlehamn, C.S.; Grifoni, A.; Dhanda, S.K.; Paul, S.; Peters, B.; Weiskopf, D.; Sette, A. A Review on T Cell Epitopes Identified Using Prediction and Cell-Mediated Immune Models for Mycobacterium tuberculosis and Bordetella pertussis. *Front. Immunol.* **2018**, *9*, 2778. [[CrossRef](#)]
61. Lindestam Arlehamn, C.S.; Lewinsohn, D.; Sette, A.; Lewinsohn, D. Antigens for CD4 and CD8 T cells in tuberculosis. *Cold Spring Harb. Perspect. Med.* **2014**, *4*, a018465. [[CrossRef](#)]
62. Gagneux, S.; Small, P.M. Global phylogeography of Mycobacterium tuberculosis and implications for tuberculosis product development. *Lancet Infect. Dis.* **2007**, *7*, 328–337. [[CrossRef](#)]
63. Day, T.A.; Penn-Nicholson, A.; Luabeya, A.K.K.; Fiore-Gartland, A.; Du Plessis, N.; Loxton, A.G.; Vergara, J.; Rolf, T.A.; Reid, T.D.; Toefy, A.; et al. Safety and immunogenicity of the adjunct therapeutic vaccine ID93 + GLA-SE in adults who have completed treatment for tuberculosis: A randomised, double-blind, placebo-controlled, phase 2a trial. *Lancet Respir. Med.* **2020**, *9*, 373–386. [[CrossRef](#)] [[PubMed](#)]

64. Baldwin, S.L.; Ching, L.K.; Pine, S.O.; Moutaftsi, M.; Lucas, E.; Vallur, A.; Orr, M.T.; Bertholet, S.; Reed, S.G.; Coler, R.N. Protection against tuberculosis with homologous or heterologous protein/vector vaccine approaches is not dependent on CD8+ T cells. *J. Immunol.* **2013**, *191*, 2514–2525. [[CrossRef](#)] [[PubMed](#)]
65. Lu, Y.-J.; Barreira-Silva, P.; Boyce, S.; Powers, J.; Cavallo, K.; Behar, S.M. CD4 T cell help prevents CD8 T cell exhaustion and promotes control of Mycobacterium tuberculosis infection. *Cell Rep.* **2021**, *36*, 109696. [[CrossRef](#)]
66. Irvine, E.B.; O'Neil, A.; Darrah, P.A.; Shin, S.; Choudhary, A.; Li, W.; Honnen, W.; Mehra, S.; Kaushal, D.; Gideon, H.P.; et al. Robust IgM responses following intravenous vaccination with Bacille Calmette-Guérin associate with prevention of Mycobacterium tuberculosis infection in macaques. *Nat. Immunol.* **2021**, *22*, 1515–1523. [[CrossRef](#)]
67. Orr, M.T.; Beebe, E.A.; Hudson, T.E.; Argilla, D.; Huang, P.-W.D.; Reese, V.A.; Fox, C.B.; Reed, S.G.; Coler, R.N. Mucosal delivery switches the response to an adjuvanted tuberculosis vaccine from systemic TH1 to tissue-resident TH17 responses without impacting the protective efficacy. *Vaccine* **2015**, *33*, 6570–6578. [[CrossRef](#)] [[PubMed](#)]
68. Pilkington, E.H.; Suys, E.J.; Trevaskis, N.L.; Wheatley, A.K.; Zukancic, D.; Algarni, A.; Al-Wassiti, H.; Davis, T.P.; Pouton, C.W.; Kent, S.J.; et al. From influenza to COVID-19: Lipid nanoparticle mRNA vaccines at the frontiers of infectious diseases. *Acta Biomater.* **2021**, *131*, 16–40. [[CrossRef](#)]
69. Mulligan, M.J.; Lyke, K.E.; Kitchin, N.; Absalon, J.; Gurtman, A.; Lockhart, S.; Neuzil, K.; Raabe, V.; Bailey, R.; Swanson, K.A.; et al. Phase I/II study of COVID-19 RNA vaccine BNT162b1 in adults. *Nature* **2020**, *586*, 589–593. [[CrossRef](#)] [[PubMed](#)]
70. Polack, F.P.; Thomas, S.J.; Kitchin, N.; Absalon, J.; Gurtman, A.; Lockhart, S.; Perez, J.L.; Pérez Marc, G.; Moreira, E.D.; Zerbini, C.; et al. Safety and Efficacy of the BNT162b2 mRNA Covid-19 Vaccine. *N. Engl. J. Med.* **2020**, *383*, 2603–2615. [[CrossRef](#)]
71. Anderson, E.J.; Roupshael, N.G.; Widge, A.T.; Jackson, L.A.; Roberts, P.C.; Makhene, M.; Chappell, J.D.; Denison, M.R.; Stevens, L.J.; Pruijssers, A.J.; et al. Safety and Immunogenicity of SARS-CoV-2 mRNA-1273 Vaccine in Older Adults. *N. Engl. J. Med.* **2020**, *383*, 2427–2438. [[CrossRef](#)]
72. Baden, L.R.; El Sahly, H.M.; Essink, B.; Kotloff, K.; Frey, S.; Novak, R.; Diemert, D.; Spector, S.A.; Roupshael, N.; Creech, C.B.; et al. Efficacy and Safety of the mRNA-1273 SARS-CoV-2 Vaccine. *N. Engl. J. Med.* **2021**, *384*, 403–416. [[CrossRef](#)] [[PubMed](#)]

Disclaimer/Publisher's Note: The statements, opinions and data contained in all publications are solely those of the individual author(s) and contributor(s) and not of MDPI and/or the editor(s). MDPI and/or the editor(s) disclaim responsibility for any injury to people or property resulting from any ideas, methods, instructions or products referred to in the content.